The Effect of Proton Irradiation on the Micromechanical hardness of Ferritic/Martensitic Steel

Jeonghyeon Lee, Tae Yong Kim, and Ji Hyun Kim*
Department of Nuclear Engineering, School of Mechanical, Aerospace and Nuclear Engineering, Ulsan National Institute of Science and Technology (UNIST), Ulju-gun, Ulsan 44919, Republic of Korea
*Corresponding author: kimjh@unist.ac.kr

1. Introduction

Liquid metal fast breeder reactors (LMFBRs) such as the sodium-cooled fast reactor (SFR) and the lead-cooled fast reactor (LFR) are candidates among GEN-IV nuclear energy systems. Among the various liquid metals that can be used to a primary coolant materials, and sodium is a world widely used coolant in the design of Gen-IV reactors [1]. As a coolant for fast reactor systems, liquid sodium provides some advantages over liquid lead or lead-bismuth eutectic (LBE). The sodium has 100 times more effective heat transfer medium compared to water and wide temperature margin about 400 ℃ to boiling. Sodium features a reasonably low melting temperature, but also a low boiling point (883 ℃), which raises safety concerns regarding unprotected transients leading to a coolant heatup. And, LBE or lead coolant velocity is limited by erosion concerns of protective oxide layers to about 2.5–3.0 m/s. Typical sodium velocities are up to 8–10 m/s, hence lead has, in practice, a lower heat removal capacity. And, These features together with the higher flow velocity of sodium lead to higher linear power being available and a lower pitch to diameter ratio required [2,3].

Irradiation swelling resistance and stability of mechanical properties are very important issues for development of fast reactor cladding materials at elevated temperature under fast neutron irradiation conditions. Austenitic steels such as 304 and 316 stainless steels have been used as the first generation fast reactor cladding materials, and then advanced austenitic steels which are superior to swelling characteristics have been developed and used. However, in Generation IV reactors 9–12% chromium ferritic/martensitic steels (FMS) such as HT9 and Gr.92 are being considered as sodium fast reactor cladding materials because of their excellent void swelling resistance although their high temperature strength is inferior to that of austenitic steels [4].

While nuclear reactor is running, the structure material of a cladding materials will face neutron and multiple types of ion beam irradiations, which will induce the structure damage in the cladding [5–7]. Proton irradiation has been used in the past decades to reproduce neutron damage, and protons have a scattering cross-section higher than fast neutrons, and it leading to a displacement rate for nuclear material research [8–10]. Besides, The reduction of total elongation is observed to linearly increase by increasing the dose, and significant influence of liquid metal on the tensile properties [11].

In this study, FMS and irradiated FMS were tested as microhardness and observed to microstructure. The effect of irradiation on the FMS will be concluded. Especially, it is aimed to conclude the effect of irradiation conditions on the change of hardness of FMS materials.

2. Experimental

The composition of the Gr.92 used in this experiment is given in table 1. Heat treatment was performed normalizing and tempering. The both specimen was normalized at 1050 ℃ for 1 hour, followed by air cooling, then tempering at 780 ℃ for 30 min. The sample was cut into small strips with the size: 10mm×5mm×2mm and further polished successively with 320, 400, 600, and 800 grit polishing paper and diamond polishing until 1 μm. It was cleaned in an ultrasonic cleanser with ethanol, acetone, and distilled water in sequence.

Table 1. Chemical composition of the test material (wt.%)

	C	Si	Mn	Cr	Ni	Mo	W	V
Gr.92	0.087	0.21	0.41	8.69	0.13	0.38	1.62	0.18

The proton irradiation experiments were carried out in TR23 (20 MeV) accelerator in KOMAC (Korea Multi-purpose Accelerator Complex), gyeong-ju, Korea. The beam dump of KOMAC is located the photon production downstream are for a continuous absorption of the generated beam energy [12].

In the case of irradiation with 3 MeV protons, the proton fluences were 5×10^{15}#/cm^2 and 10^{16}#/cm^2, respectively. Those fluences were condition for maximum terms for highest displacement per atom at KOMAC. The stability of the current was within ±5%. The largest average current is 0.6mA, pulse width is 0.05 ms. The total damage and depth of stopping range in the sample, calculated through the Stopping and Range of

Ions in Matter (SRIM) code. The temperature of irradiation environment is room temperature, and dose flux is 10^{10}p/cm^2 each pulse. And the average proton irradiation dose area was measured at the center of the film with an area of 5cm × 5cm.

In the case of irradiation with 3 MeV protons, the proton fluences were 5×10^{15}#/cm^2 and 10^{16}#/cm^2, respectively. Those fluences were condition for maximum.

The ex situ investigation was performed to characterize the dislocation analysis of the specimen using FEI Nanonova 230 field emission scanning electron microscope, and JEOL JEM-2100F transmission electron microscope in coincidence. The focused ion beam milling method was employed using a Quanta3D Dual-Beam SEM to prepare the TEM specimen. The TEM sample position is located under the 20 μm from surface.

Room temperature microhardness measurements were carried out using Vickers Test using a diamond Vickers indenter and a load of 1 kgf. An average of five indentations was made on each sample and their average value was noted. The hardness (HV) was calculated from

$$\mathrm{HV} = \frac{\mathrm{F}}{\mathrm{A}} = \frac{1.8544F}{d^2}\ [\frac{\mathrm{kgf}}{\mathrm{mm}^2}]$$

where F is in kgf and d is in millimeters.

3. Results and Discussion

3.1 Irradiation result

Irradiations were conducted using 3 MeV protons, which have a penetration distance of 40 μm in stainless steel, to ensure that there was no implantation within the 30 μm sample. An example of the hydrogen profile and dpa profile calculated by the SRIM code is shown in below graph. The damage profile of SRIM simulation is illustrated in Fig.1. The damage profile was fairly flat at an average of 3×10^{-5} displacements/angstrom-ion.

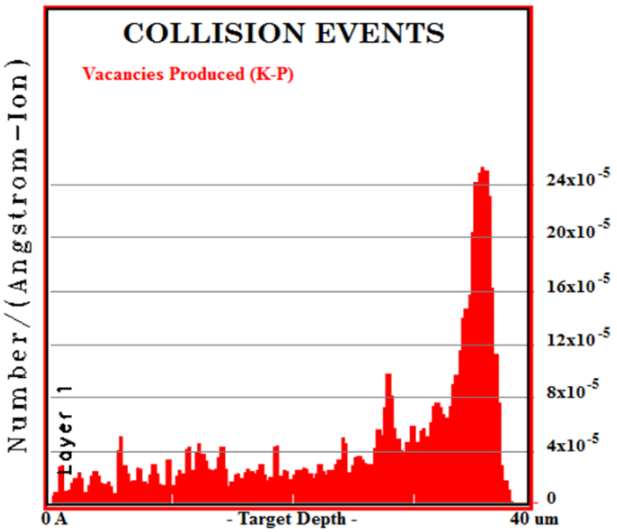

Fig. 1. SRIM result of 3MeV proton beam incident on Gr.92 target. Damage peak occurs around 38 μm into the sample. Nominal sample thickness of 30 μm was used to avoid the damage peak and any proton implantation,

3.2 Roughness change from irradiation

Figure 2 shows the atomic forced microscopy (AFM) photographs of surface morphology of specimen before and after H+ ion irradiation. It could be observed from the figure that, after irradiation, both the surface projections and the rms roughness of specimen increased. The evolution of ion beam irradiated solid surface was the result of a competition between the roughening process caused by ion bombardment and the smoothing process caused by material transport. It was clear that the roughening process caused by ion bombardment played a dominant role [13]. The experiment data in such shallow indentation depth may have been affected by the surface conditions, such as surface roughness.

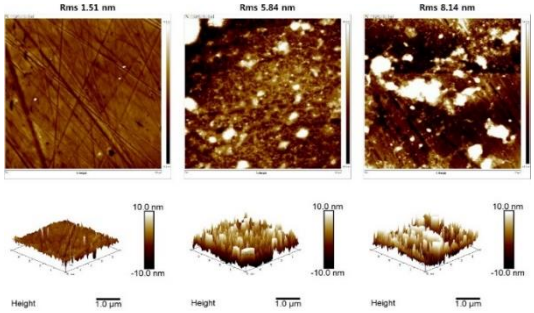

Fig. 2. AFM micrographs showing the change in surface morphology for specimen irradiated by protons with various fluences.

3.3 Irradiation damage in the absence of dislocations

These and other studies on various steels such as austenitic steel and ferritic/martensitic steel subjected to a wide range of ion irradiation conditions seem to indicate that, similar to neutron irradiation, proton irradiation induces mainly dislocation and dislocation loops in steels. The dislocation channels are formed, dislocation slip is largely confined to the channels by the harder matrix, leading to larger slip steps.

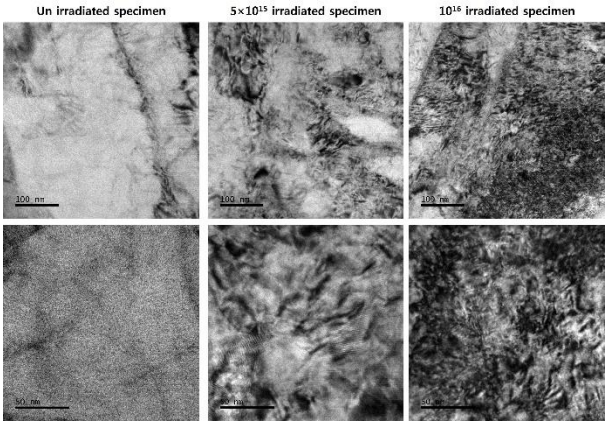

Fig. 3. TEM images of unirradiated specimen and irradiated specimen defects such as dislocation observed at 5×10^{15}#/cm^2 and 10^{16}#/cm^2

3.4 Irradiation hardening

Figure 4 shows the Comparison of hardness of Gr.92 specimen before and after proton irradiation. A significant hardness change was observed for irradiated specimens at indentation depths. After irradiation to 5×10^{15}#/cm^2 and 10^{16}#/cm^2, the microhardness increased to 90.2 HV and 230HV, respectively. The hardness was not affected by grain size change in irradiation environment. The micro-indentation was less than the grain size of either condition.

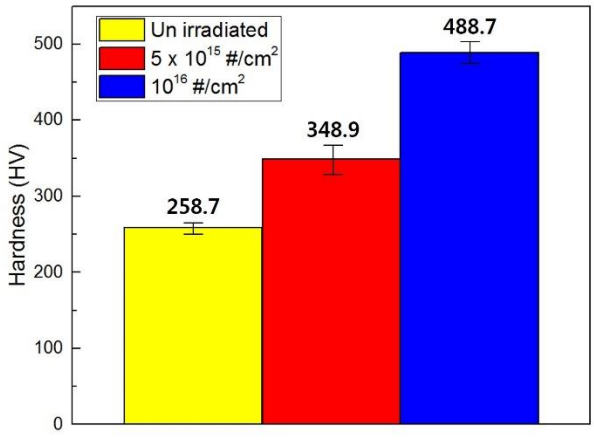

Fig. 4. Comparison of hardness of Gr.92 specimen before and after proton irradiation.

4. Conclusions

In this study, as-received Gr.92 and irradiated Gr.92 specimen were examined Vickers hardness measurement and observed microstructure. The microstructure results reveal the information for the effect of irradiation, effect of roughness change and effect of dislocation density.

i. From the SRIM result, penetration distance of 40 μm in stainless steel and nominal sample thickness of 30 μm was used to avoid the damage peak and any proton implantation
ii. From the microstructural evaluation, the evolution of ion beam irradiated solid surface was the result of a competition between the roughening process caused by ion bombardment and the smoothing process caused by the material transport.
iii. Irradiation conditions seem to indicate that, similar to neutron irradiation, proton irradiation induces mainly dislocation and dislocation loops in steels.
iv. A significant hardness change was observed for irradiated specimens at indentation depths.

ACKNOWLEDGEMENTS

This work was supported by the National Nuclear R&D program funded by Ministry of Science, ICT and Future Planning, and by the National Nuclear R&D program (NRF-2016M2B2A9A0294486) organized by the National Research Foundation (NRF) of South Korea in support of the Ministry of Science, ICT and Future Planning.

REFERENCES

[1] S.H. Shin, S.H. Kim, J.H. Kim, J. Nucl. Mater. 450 (2014) 314.
[2] J. Carlsson, H. Wider, Comparison of sodium and lead-cooled fast reactors regarding reactor physics aspects , severe safety and economical issues, 236 (2006) 1589.
[3] P. Mazgaj, P. Darnowski, S. Gurgacz, M. Lipka, K. Dziubanii, Comparison of Simple Design of Sodium and Lead Cooled Fast Reactor Cores, 94 (2014) 16.
[4] T. Furukawa, S. Kato, E. Yoshida, J. Nucl. Mater. 392 (2009) 249.
[5] J.A. Jung, S.H. Kim, S.H. Shin, I.C. Bang, J.H. Kim, J. Nucl. Mater. 440 (2013) 596
[6] J.H. Kim, S.H. Kim, J. Nucl. Mater. 443 (2013) 112
[7] M.C. Billone, T. a. Burtseva, R.E. Einziger, J. Nucl. Mater. 433 (2013) 431
[8] S.H. Shin, J.H. Lee, J.K. Lee, J. Lim, S. Choi, G. Kim, J.H. Kim, J. Electrochem. Soc. 162 (2015) B152
[9] J. Lee, S.H. Shin, J.K. Lee, S. Choi, J.H. Kim, J. Power Sources. 307 (2016) 526

[10] W.J.S. Yang, J. Nucl. Mater. 158 (1988) 71
[11] G.E. Lucas, M. Surprenant, J. Dimarzo, G.J. Brown, J. Nucl. Mater. 101 (1981) 78
[12] J.J. Kai, W.I. Huang, H.Y. Chou, J. Nucl. Mater. 170 (1990) 193